J Mater Sci (2010) 45:3757–3767
DOI 10.1007/s10853-010-4425-4

The effect of temperature on fatigue damage of FRP composites

H. Mivehchi · A. Varvani-Farahani

Received: 19 November 2009 / Accepted: 17 March 2010 / Published online: 2 April 2010

Abstract The present study intends to investigate the effect of temperature on cumulative fatigue damage (D) of laminated fibre-reinforced polymer (FRP) composites. The effect of temperature on fatigue damage is formulated based on Ramkrishnan–Jayaraman and Varvani-Farahani–Shirazi residual stiffness fatigue damage models. The models are further developed to assess the fatigue damage of FRP composites at various temperatures (T). This task is fulfilled by formulating the temperature dependency of Young's modulus (E) and ultimate tensile strength (σ_{ult}) as the inputs of the models. Temperature-dependant parameters of Young's modulus and ultimate tensile strength are found to be in good agreement with the experimentally obtained data when used for unidirectional, cross-ply and quasi-isotropic FRP laminates. The proposed fatigue damage model is evaluated using six sets of fatigue damage data. The proposed temperature-dependent model was also found promising to predict the fatigue damage of unidirectional (UD) and orthogonal woven FRP composites at different temperatures.

Introduction

The major fatigue models and life time methodologies for fibre-reinforced polymer (FRP) composites are classified into three categories: (i) fatigue life models, which do not take into account the actual degradation mechanisms, such as matrix cracks and fibre fracture, but use S–N curves or Goodman-type diagrams and introduce some fatigue failure criteria [1–4], (ii) phenomenological models for residual stiffness/strength [1, 5–8] and (iii) progressive damage models which analyze the fatigue damage based on some measurable damage variables such as transverse matrix cracks and delamination size [1, 9–11].

The fatigue damage model employed in this study is constructed based on stiffness degradation of materials over life cycles. Stiffness degradation damage models [5–7] are reliable approaches relating damage progress of FRP composite material properties, including the properties of the matrix, fibre and fibre–matrix interface as the number of stress cycles progresses. Ramkrishnan–Jayaraman and Varvani-Farahani–Shirazi damage models [5, 6] are used as the backbone of analysis in this paper. Mechanical properties of FRP composite laminates including their micro-constituents are further formulated as a function of operating temperatures. Temperature-dependent parameters of Young's modulus and ultimate tensile strength as inputs of the damage model characterize the damage of FRP composite specimens at various operating temperatures.

Fatigue damage analysis of FRP composites

The progressive development of damage during fatigue life can be overviewed with the aid of Fig. 1, which represents the development of damage during the fatigue life of unidirectional composite materials [6].

In region I, multiple crack initiations within the matrix are grouped together during the first 20% of the fatigue life. Region II commences as matrix cracks reach the vicinity of fibre. As the number of cycles increases, the crack grows along the fibre–matrix interface. This region is characterized with a larger life span and a lower slope of damage

H. Mivehchi (✉) · A. Varvani-Farahani
Department of Mechanical & Industrial Engineering, Ryerson University, 350 Victoria Street, Toronto, ON M5B 2K3, Canada
e-mail: hmivehch@ryerson.ca

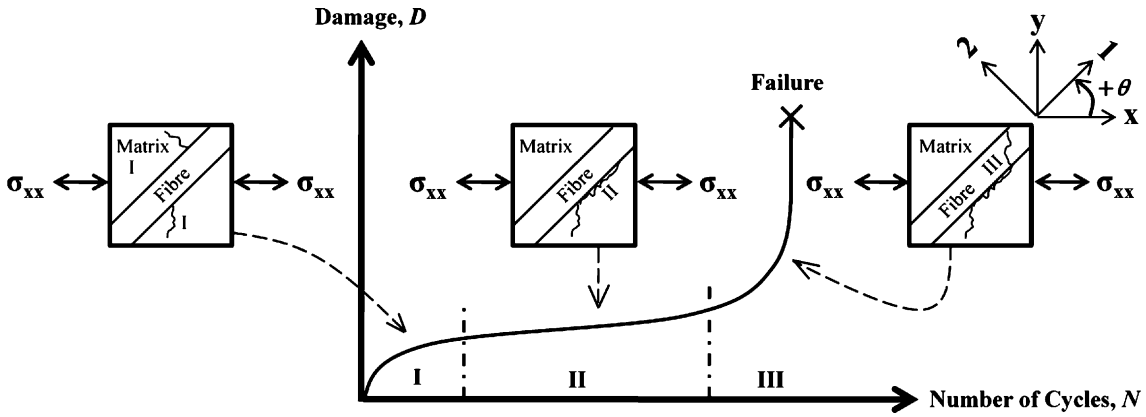

Fig. 1 Three regions of cracking mechanism in unidirectional composites [6]

progress. In region III, with a shorter life span, fibre breakage occurs shortly after damage has been accumulated during regions I and II [6].

Any physically based damage model for a composite must use contributions from individual constituents as building blocks to determine the overall damage to the composite. The peculiarity of damage is that the three constituents of FRP composites (matrix, fibre–matrix interface and fibre) do not fail simultaneously. This is explained by their differing mechanical properties [6]. Amongst different types of fatigue damage models, the concept of cumulative damage may be used as the most suitable approach to analyze and predict the fatigue behaviours of composite materials. It has been observed that the cumulative fatigue damage of composite materials can be measured in terms of stiffness reduction. Therefore, the quantitative evaluation of the fatigue damage can be shown as

$$D = 1 - \frac{E_N}{E_0} \tag{1}$$

where D is cumulative fatigue damage, E_0 is the initial Young's modulus of the undamaged material, and E_N is the Young's modulus of the damaged material in cycle N. Thus, the extent of damage can be quantified by measuring the Young's modulus of the material. It is concluded from Eq. 1 that D varies between 0 and 1. When there is no damage, D equals 0, and when the material is fully damaged D becomes 1.

The mechanical behaviour of a composite material depends upon the response of its constituents, namely, the fibre, the matrix and their interface. Ramakrishnan and Jayaraman [5] have developed a stiffness-based damage model based on individual constituents as building blocks to determine the overall damage to the composite. In their model, a combination of logarithmic and linear decay functions of time (or cycles) was associated with the stiffness drops for the different damage processes. The total damage (D) as a function of the number of fatigue cycles (N) was described as

$$D = \left\{\frac{E_m V_m}{E_c}(1 - f^*)\frac{\ln(N+1)}{\ln(N_f)}\right\} + \left\{\frac{E_m V_m}{E_c} f^* \left(\frac{N}{N_f}\right)\right\} + \left\{\frac{E_f V_f}{E_c}\left(1 - \frac{\sigma_{appl}}{\sigma_{ult}}\right)\frac{\ln\left(1 - \frac{N}{N_f}\right)}{\ln\left(\frac{1}{N_f}\right)}\right\} \tag{2}$$

where N_f is the fatigue life or number of cycles to failure, E_m is the Young's modulus of matrix, E_f is the Young's modulus of fibre, V_m is the volume fraction of matrix, V_f is the volume fraction of fibre, E_c is the Young's modulus of composite, f^* is the fibre/matrix interface strength parameter, $(0 \le f^* \le 1)$, σ_{appl} is the applied tensile fatigue stress, and σ_{ult} is the ultimate tensile stress.

The change of the fibres angle in respect to loading direction in a composite can change the strength of the composite. As the angle θ is increased from 0° to 90°, the stiffness of the composite is decreased. Moreover, the effect of mean stress on fatigue damage is also crucially important. Varvani-Farahani and Shirazi [6] have further developed the Ramakrishnan–Jayaraman fatigue damage model to include the effect of fibre orientation and mean stress as

$$D = \left\{\left(1 - \frac{E_f V_f \cos\theta}{E_c}\right)(1 - f^*)\frac{\ln(N+1)}{\ln(nN_f)}\right\} + \left\{\left(1 - \frac{E_f V_f \cos\theta}{E_c}\right) f^* \left(\frac{N}{nN_f}\right)\right\} + \left\{\frac{E_f V_f \cos\theta}{E_c}\left(1 - \frac{\sigma_{max}(1-R)}{2\sigma_{ult}}\right)\frac{\ln\left(1 - \frac{N}{nN_f}\right)}{\ln\left(\frac{1}{nN_f}\right)}\right\} \tag{3}$$

where θ is the angle between the fibre and the load direction, σ_{max} is the maximum fatigue stress, and R is the stress ratio ($\sigma_{min}/\sigma_{max}$).

In Eq. 3, term n corresponds to the percentage of drop in stiffness assumed and specified for a fatigue test. For instance, by considering the degradation up to the 60% of the real damage life, term $n = (0.6)^{-1} = 1.67$. Then, the number of cycles to failure is estimated as $nN_f = 1.67N_f$.

Temperature-dependant parameters in damage assessment

Fatigue damage D in Eq. 3 has been developed as a function of the maximum applied stress σ_{max}, number of loading cycles N, load or stress ratio R and material and structural properties, such as Young's modulus E, volume fraction V and fibre orientation θ. The equation can be further modified including the effect of temperature T, i.e.;

$$D = D(\sigma_{max}, N, R, E, V, \theta, T, \ldots) \tag{4}$$

In Eq. 3, three parameters including Young's modulus of the composite, E_c, composite ultimate tensile strength, σ_{ult}, and the fatigue life of composite, N_f, were found to be temperature-dependent. Substituting the temperature-dependent parameters in Eq. 3, the fatigue damage equation can be expressed as

$$\begin{aligned} D = & \left\{ \left(1 - \frac{E_f V_f \cos\theta}{E_c(T)} \right) (1 - f^*) \frac{\ln(N+1)}{\ln(nN_f(T))} \right\} \\ & + \left\{ \left(1 - \frac{E_f V_f \cos\theta}{E_c(T)} \right) f^* \left(\frac{N}{nN_f(T)} \right) \right\} \\ & + \left\{ \frac{E_f V_f \cos\theta}{E_c(T)} \left(1 - \frac{\sigma_{max}(1-R)}{2\sigma_{ult}(T)} \right) \frac{\ln\left(1 - \frac{N}{nN_f(T)}\right)}{\ln\left(\frac{1}{nN_f(T)}\right)} \right\} \end{aligned} \tag{5}$$

To recognize the effect of temperature in Eq. 5, the functions of $E_c(T)$, $\sigma_{ult}(T)$ and $N_f(T)$ are required to be characterized.

The effect of temperature on the static and fatigue strengths of FRP composites and polymers has been studied by several researchers [12–16]. In these studies, either the Williams–Landel–Ferry (WLF) equation or an Arrhenius equation was employed to introduce a shift factor. The shift factor includes the effect of temperature on mechanical properties of polymers. Based on the WLF equation, the shift factor $a(T)$ is expressed as

$$\log a(T) = \frac{-C_1(T - T_0)}{C_2 + T + T_0} \tag{6}$$

where T is temperature, T_0 is the reference temperature which has typically been supposed as T_g, and the constants C_1 and C_2, originally thought to be universal constants, have been shown to vary rather slightly from polymer to polymer. A list of C_1 and C_2 for some polymers has been presented in Ref. [15]. These constants have experimentally been measured at $T_0 = T_g$. The WLF equation is usually suitable for the temperature range of $T_g < T < T_g + 100$ K [16]. Therefore, it is normally used to predict the effect of temperature on the mechanical properties of the bulk polymers in the viscoelastic and rubbery regions only. For polymers at temperatures above $T_g + 100$ K, the Arrhenius equation is used

$$\log a(T) = \frac{\Delta H}{2.303 G_C} \left(\frac{1}{T} - \frac{1}{T_0} \right) \tag{7}$$

where G_C is the gas constant, 8.314 (J/K mol), ΔH (J/mol) is the viscoelastic activation energy of the polymer, and T_0 is the reference temperature where $T_0 \neq T_g$. The Arrhenius equation is usually applicable for rubber-like and liquid polymers.

The disadvantages of both WLF and Arrhenius equations are that: first, they are usually suitable for bulk polymers not composites; second, they are normally applicable in temperatures above the glass transition temperature of the polymer; and third, to obtain the constants in either equation, many experimental measurements are required. Therefore, to predict the mechanical properties of FRP laminates at various temperatures, it is essential to develop a model which is applicable to the composites, valid to a wider range of temperatures and requires less experimental measurements.

Temperature-dependant relations for monotonic properties

In viscoelastic polymers, the shift factor $a(T)$ is usually employed to predict the behaviour of the tensile viscosity $\eta(T)$ of a polymer at different temperatures as

$$\eta(T) = a(T)\eta(T_0) \tag{8}$$

where $\eta(T_0)$ is the tensile viscosity at the reference temperature, and $a(T)$ is the shift factor obtained from Eqs. 6 or 7. It is obvious that a relation such as Eq. 8 can be written for any mechanical property of a material. Therefore, by rewriting Eq. 8 for the ultimate tensile strength and the Young's modulus of laminated FRP composites, we have

$$\sigma_{ult}(T) = a_\sigma(T)\sigma_{ult}(T_0) \tag{9}$$

and

$$E(T) = a_E(T)E(T_0) \tag{10}$$

In the above two equations, $\sigma_{ult}(T)$ and $E(T)$ are, respectively, the ultimate tensile strength and the Young's modulus at an arbitrary temperature; $\sigma_{ult}(T_0)$ and $E(T_0)$ are the values of the physical parameters at the reference temperature, and $a_\sigma(T)$ and $a_E(T)$ are the shift factors.

Equations 8–10 are employed to identify material properties at any arbitrary temperature. These equations require both the reference temperature and the shift factor as known parameters. To formulate $\sigma_{ult}(T)$ and $E(T)$ in laminated FRP composites, a new relation for the shift factor, $a(T)$, is proposed as follows:

$$a(T) = \left[1 - \frac{C}{\ln\left(1 - \frac{T_0}{T_m}\right)} \ln\left(\frac{\left(1 - \frac{T}{T_m}\right)}{\left(1 - \frac{T_0}{T_m}\right)}\right)\right] \tag{11}$$

where T is temperature, T_0 denotes the reference temperature and T_m is the polymer melting temperature of the composites, all in Kelvin. Constant C in Eq. 11 corresponds to the sensitivity of material or mechanical property to temperature variation and is defined based on the mechanical property as Eqs. 12 and 13

$$C_\sigma = \left(\frac{\sigma_{ult}(0)}{\sigma_{ult}(T_0)} - 1\right) \tag{12}$$

and

$$C_E = \left(\frac{E(0)}{E(T_0)} - 1\right) \tag{13}$$

In these equations, $\sigma_{ult}(0)$ and $E(0)$ are the ultimate tensile strength and the Young's modulus at absolute zero temperature (0 K = −273 °C), respectively. Terms $\sigma_{ult}(T_0)$ and $E(T_0)$ correspond to values of the physical parameters at the reference temperature. In both cases, by knowing the amount of the mechanical properties at 0 K and T_0 (T_0 is normally assumed as room temperature) the corresponding constant is achieved.

The measurement of $\sigma_{ult}(0)$ or $E(0)$ at absolute zero (the coldest temperature) is theoretically possible. The temperatures of liquid oxygen, nitrogen, hydrogen and helium are about 90, 77, 22 and 4 K, respectively. Using advanced cryogenic equipment, temperatures as low as 4 K (using liquid helium) are achieved to obtain $\sigma_{ult}(4)$ and $E(4)$, which are close enough to values of $\sigma_{ult}(0)$ and $E(0)$. Based on Eqs. 11–13, Eqs. 9 and 10 can be rewritten as follows:

$$\sigma_{ult}(T) = \sigma_{ult}(T_0)\left[1 - \frac{\left(\frac{\sigma_{ult}(0)}{\sigma_{ult}(T_0)} - 1\right)}{\ln\left(1 - \frac{T_0}{T_m}\right)} \ln\left(\frac{\left(1 - \frac{T}{T_m}\right)}{\left(1 - \frac{T_0}{T_m}\right)}\right)\right] \tag{14}$$

and

$$E(T) = E(T_0)\left[1 - \frac{\left(\frac{E(0)}{E(T_0)} - 1\right)}{\ln\left(1 - \frac{T_0}{T_m}\right)} \ln\left(\frac{\left(1 - \frac{T}{T_m}\right)}{\left(1 - \frac{T_0}{T_m}\right)}\right)\right] \tag{15}$$

Equations 14 and 15 are the models which predict the amount of the ultimate tensile strength and the Young's modulus of laminated FRP composites at different temperatures. In Eqs. 12 and 13, where $\sigma_{ult}(0) \geq \sigma_{ult}(RT)$ and $E(0) \geq E(RT)$, the constants C_σ and C_E vary between 0 and 1 for almost all laminated FRP composites. In these cases, Eqs. 14 and 15 are plotted as the diagram presented in Fig. 2.

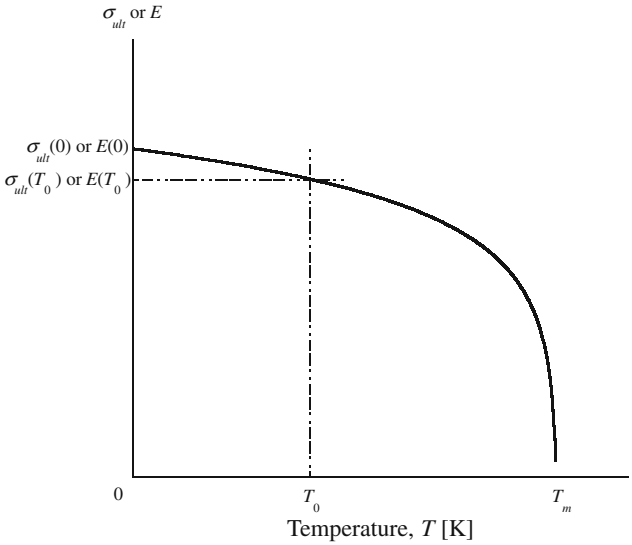

Fig. 2 A typical curve of σ_{ult}–T or E–T plotted with Eq. 14 or 15

To implement the effect of temperature in fatigue damage Eq. 5, the temperature dependant parameters of $\sigma_{ult}(T)$ and $E(T)$ or $E_c(T)$ have been formulated. The proposed relationships for the parameters have been developed in Eqs. 14 and 15. Fatigue life data N_f obtained at temperature T was used as an input of the damage equation. Therefore, considering the parameters, fatigue damage Eq. 5 is given as

$$\begin{aligned} D = &\left\{\left(1 - \frac{F}{E_c(T)}\right)(1 - f^*)\frac{\ln(N+1)}{\ln(nN_f)}\right\} \\ &+ \left\{\left(1 - \frac{F}{E_c(T)}\right)f^*\left(\frac{N}{nN_f}\right)\right\} \\ &+ \left\{\frac{F}{E_c(T)}\left(1 - \frac{\sigma_{max}(1-R)}{2\sigma_{ult}(T)}\right)\frac{\ln\left(1 - \frac{N}{nN_f}\right)}{\ln\left(\frac{1}{nN_f}\right)}\right\} \end{aligned} \tag{16}$$

Term F in Eq. 16 varies based on composite laminate lay-up. For unidirectional composites, term F extracted from the rule of mixtures becomes $E_f V_f \cos(\theta)$. For orthogonal woven composites, the rule of mixtures results in $F = K_f E_f V_f$. Note that $V_f^* = K_f V_f$ corresponds to the volume fraction of fibres which are aligned in the loading direction.

Similar to the previously developed fatigue damage formulations, Eq. 16 holds terms of damage in three regions of the matrix, matrix–fibre interface and fibre. Using Eq. 16, the procedure of damage analysis includes:

(i) Define input parameters of E_f, V_f, V_f*, $E_c(T)$, f*, $\sigma_{ult}(T)$, σ_{max}, R, n, and N_f.
(ii) Calculate the values of damage cycle-by-cycle.
(iii) Calculate the total damage over fatigue life cycles.

Evaluation of the temperature-dependent parameters

Evaluation of temperature-dependent monotonic relations

Experimental data extracted from the literature [17–20] have been used to evaluate the formulations proposed for the ultimate tensile strength and Young's modulus. The tested materials, the type of plies and laminates, the reported fibre volume fraction of some specimens and the amount of the mechanical properties at room temperature have been listed in Tables 1 and 3. The following section presents two extensive sources of experimental data used in this paper.

Jen et al. [20] tensile tested samples made of graphite/PEEK (AS-4/PEEK) prepregs with different lay-ups of cross-ply $[0/90]_{4S}$ and quasi-isotropic $[0/+45/90/-45]_{2S}$ laminates. After curing, the laminates were cooled down at room temperature (RT) and taken out from the hot press. A cutting machine with diamond blade and water cooling was used to cut the laminates into $L = 240$ mm, $W = 25.4$ mm and $t = 2$ mm coupons, according to ASTM D3039-93. Copper plate was considered as end tabs by NP-50 two-component adhesive. The fibre volume fraction of the specimens was reported to be about 61%. The tension tests on the specimens were performed at RT (25 °C), 50, 75, 100, 125,150 and 175 °C.

Shen and Springer [17, 18] have measured ultimate tensile strength and buckling modulus of a special kind of graphite/epoxy specimens called Thornal 300/Fiberite 1034 at different temperatures. The size of the specimens in the tension test was reported as $L = 101$ mm, $W = 12.7$ mm and $t = 0.9$ mm, and the size in the buckling tests was reported as $L = 36$–318 mm, $W = 4.76$ mm and $t = 0.9$ mm. Shen and Springer have also evaluated the ultimate tensile strength and Young's modulus variations with temperature using different sets of data available in the literature. The summary of the test data is discussed as follows: Thornel 300/Narmco 5208 was tensile tested at a temperature range between 300 and 450 K, reported by Hofer et al. [21] and Husman [22]. Hertz [23] performed monotonic tests on HT-S/(8183/137-NDA-BF_3:MEA) at various temperatures of 200–450 K. The experimental measurements of Browning et al. [24] on the influence of temperature on σ_{ult} for Herculus AS-5/3501 ranged from 300 to 425 K. Further experiments were conducted to obtain the effect of temperature on σ_{ult} for boron/Narmco 5505 by Kaminski [25]. In addition to σ_{ult} experiments, Hofer et al. [21] conducted a new sets of tensile tests to evaluate E with temperature change between 300 and 450 K.

Evaluation of $\sigma_{ult}(T)$ and $E(T)$ results

To calculate $\sigma_{ult}(T)$ and $E(T)$ using Eqs. 14 and 15 the following parameters are required:

(i) The amount of σ_{ult} and E at room temperature, $\sigma_{ult}(T_0 = \text{RT})$ and $E(T_0 = \text{RT})$.
(ii) The amount of σ_{ult} and E at 0 K, $\sigma_{ult}(0)$ and $E(0)$.
(iii) Room temperature, RT, and the polymer melting point of the tested FRP laminate, T_m.

To evaluate Eqs. 14 and 15, over 10 different composite materials [17–20] were examined. All the parameters required to calculate the proposed relations were taken from the literature and are listed in Tables 1, 2, 3 and 4.

Table 1 The experimental information used for the evaluation of the proposed σ_{ult}–T relation

Composite	Reference	Plies/laminates	Fibre volume fraction, V_f (%)	Ultimate tensile strength at RT, σ_{ult} (RT) (MPa)
Boron/epoxy	[19]	0°	50	1,400 (295 K)
S-glass/epoxy	[19]	0°	–	1,600 (295 K)
E-glass/epoxy	[19]	0°	70	1,100 (295 K)
Alumina/PEEK	[19]	0°	45	800 (295 K)
AS-4/PEEK	[20]	$[0/90]_{4S}$	61	1,068.4 (298 K)
AS-4/PEEK	[20]	$[0/+45/90/-45]_{2S}$	61	730.4 (298 K)
Thornel 300/Fiberite 1034	[17]	90°	–	58.6 (300 K)
Thornel 300/Narmco 5208	[17]	90°	–	40.4 (300 K)
HT-S/(8183/137-NDA-BF_3:MEA)	[17]	90°	–	49.5 (300 K)
Herculus AS-5/3501	[17]	90°	63	54.8 (300 K)
Boron/Narmco 5505	[17]	90°	–	109.9 (300 K)

Table 2 The experimental information (extrapolated and reported) used for the evaluation of the proposed σ_{ult}–T relation

Composite	Reference	Plies/laminates	$\sigma_{ult}(0)$ (MPa) (extrapolated)	C_σ	Polymer melting point, T_m (K) (extrapolated)
Boron/epoxy	[19]	0°	1,820	0.3	450
S-glass/epoxy	[19]	0°	2,000	0.25	450
E-glass/epoxy	[19]	0°	1,320	0.2	450
Alumina/PEEK	[19]	0°	1,000	0.25	616
AS-4/PEEK	[20]	$[0/90]_{4S}$	1,496	0.4	616 (Reported)
AS-4/PEEK	[20]	$[0/+45/90/-45]_{2S}$	877	0.2	616 (Reported)
Thornel 300/Fiberite 1034	[17]	90°	82	0.4	431
Thornel 300/Narmco 5208	[17]	90°	57	0.4	532
HT-S/(8183/137-NDA-BF_3:MEA)	[17]	90°	65	0.3	457
Herculus AS-5/3501	[17]	90°	65	0.2	474
Boron/Narmco 5505	[17]	90°	143	0.3	546

Table 3 The experimental information used for the evaluation of the proposed E–T relation

Composite	Reference	Plies/laminates	Fibre volume fraction, V_f (%)	Young's Modulus at RT, E(RT) (MPa)
Boron/epoxy	[19]	0°	50	210,000 (295 K)
S-glass/epoxy	[19]	0°	–	57,000 (295 K)
E-glass/epoxy	[19]	0°	70	43,000 (295 K)
Alumina/PEEK	[19]	0°	45	90,000 (295 K)
AS-4/PEEK	[20]	$[0/90]_{4S}$	61	77,680 (298 K)
AS-4/PEEK	[20]	$[0/+45/90/-45]_{2S}$	61	55,010 (298 K)
Thornel 300/Fiberite 1034	[18]	90°	–	7,375 (300 K)
Thornel 300/Narmco 5208	[18]	90°	–	9,042 (300 K)
HT-S/(8183/137-NDA-BF_3:MEA)	[18]	90°	–	3,433 (300 K)
Courtaulds HMS/Herculus 3002M	[18]	90°	–	6,979 (300 K)

Table 4 The experimental information (extrapolated and reported) used for the evaluation of the proposed E–T relation

Composite	Reference	Plies/laminates	$E(0)$ (MPa) (extrapolated)	C_E	Polymer melting point, T_m (K) (extrapolated)
Boron/epoxy	[19]	0°	239,400	0.1	450
S-glass/epoxy	[19]	0°	62,700	0.1	450
E-glass/epoxy	[19]	0°	47,300	0.1	450
Alumina/PEEK	[19]	0°	99,900	0.1	616
AS-4/PEEK	[20]	$[0/90]_{4S}$	85,448	0.1	616 (Reported)
AS-4/PEEK	[20]	$[0/+45/90/-45]_{2S}$	60,511	0.1	616 (Reported)
Thornel 300/Fiberite 1034	[18]	90°	8,850	0.2	431
Thornel 300/Narmco 5208	[18]	90°	10,850	0.2	532
HT-S/(8183/137-NDA-BF_3:MEA)	[18]	90°	4,464	0.3	457
Courtaulds HMS/Herculus 3002 M	[18]	90°	7,677	0.1	550

The calculated mechanical properties at various operating temperatures were compared with the experimental values in Figs. 3, 4, 5 and 6. The figures show a good correlation between the experimental data and the predicted values. In the figures, the ultimate tensile strength shows a steeper decay than Young's modulus as operating temperature increases. These figures verify that the Young's modulus of on-axis composites is less sensitive to

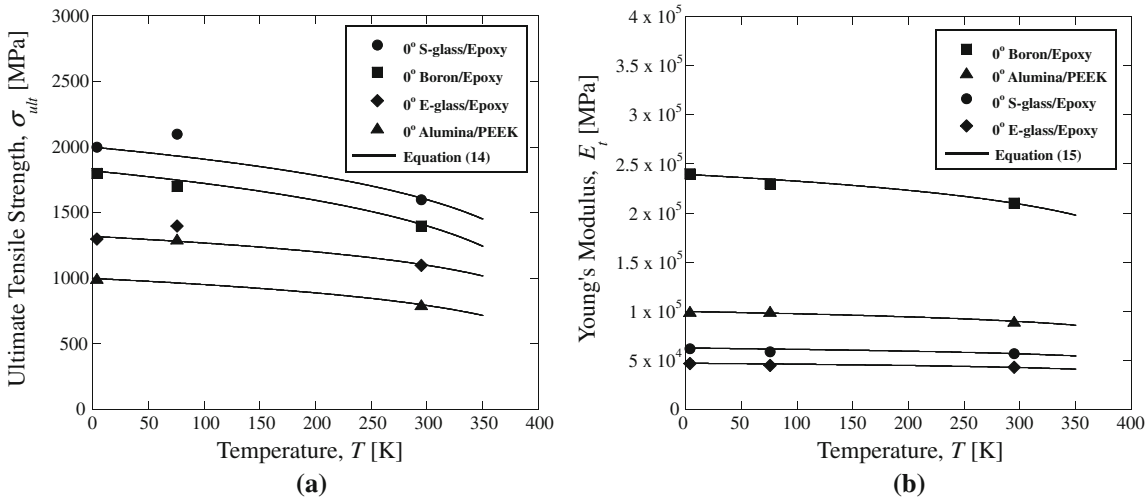

Fig. 3 (**a**) Ultimate tensile strength and (**b**) tensile modulus of different 0° FRP composites as a function of temperature. Experimental data have been extracted from Ref. [19]

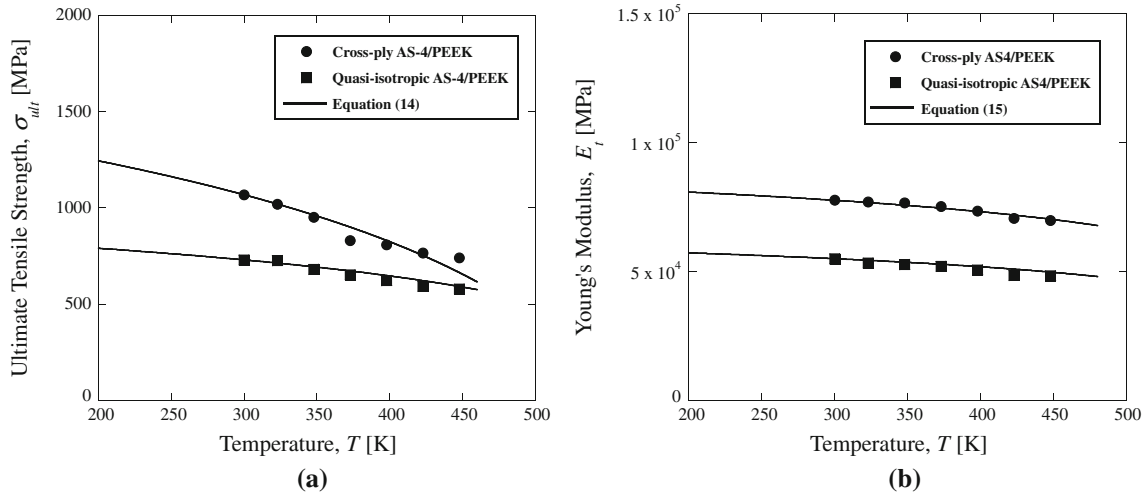

Fig. 4 (**a**) Ultimate tensile strength and (**b**) tensile modulus of $[0/90]_{4S}$ and $[0/+45/90/-45]_{2S}$ AS-4/PEEK as a function of temperature. Experimental data have been extracted from Ref. [20]

temperature change. For composites with the lay-up of 90°, the degradation of the Young's modulus becomes more pronounced as the temperature increases.

Evaluation of the fatigue damage model

Hiwa et al. [26] tested composite samples of plain-woven glass cloth (WF 350) and glass mat (MC 300S) as the reinforced fibres embedded within the matrix of polyvinyl ester resin. The FRP composite samples made by the materials have been laminated by the hand lay-up method. The number of plies in the polyvinyl ester/glass cloth and polyvinyl ester/glass mat were 5 and 3, respectively. Also, the volume fraction of the glass fibres in the cloth and mat were 48% and 35%, respectively. To measure the fatigue damage of the composites versus number of cycles at various temperatures, different fatigue tests with the loading frequency of 16.7 Hz and the stress ratio of 0 were performed on the specimens. The composites with glass cloth fibres were tested with the maximum stress of 130 MPa at RT (25 °C), 50 and 70 °C. However, the glass mat-reinforced polyvinyl ester composites were tested with the maximum stress of 90 MPa at RT (25 °C), 100 and 150 °C. In this paper, to evaluate the proposed fatigue damage model, six sets of *D*–*N* data have been extracted from the described fatigue damage experiments. A summary of the tested materials and some conditions of the fatigue tests are listed in Table 5.

In this study, to evaluate the proposed fatigue damage model of Eq. 16, its parameters have been extracted from

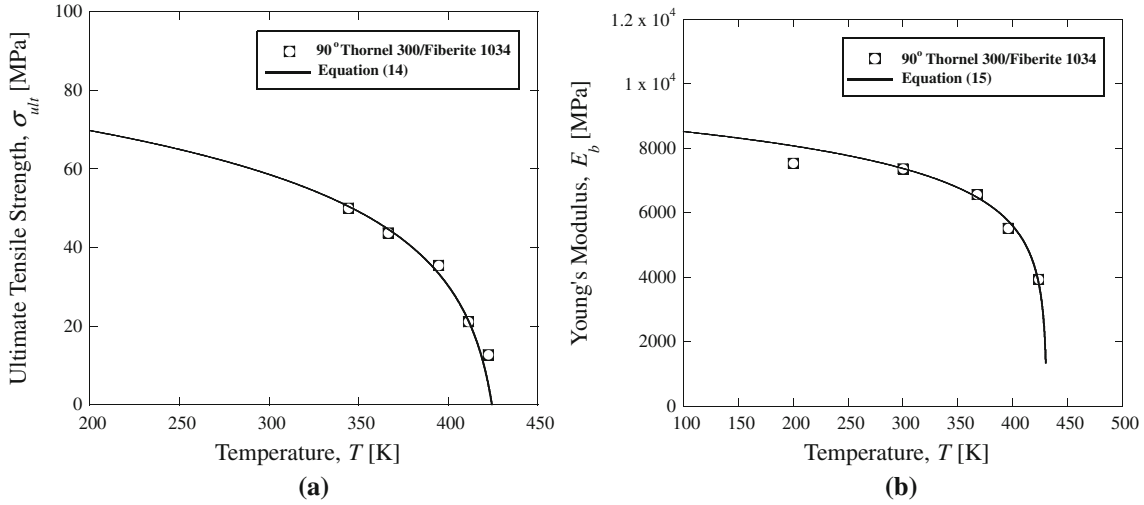

Fig. 5 (**a**) Ultimate tensile strength and (**b**) buckling modulus of 90° Thornel 300/Fiberite 1034 as a function of temperature. Experimental data have been extracted from Refs. [17, 18]

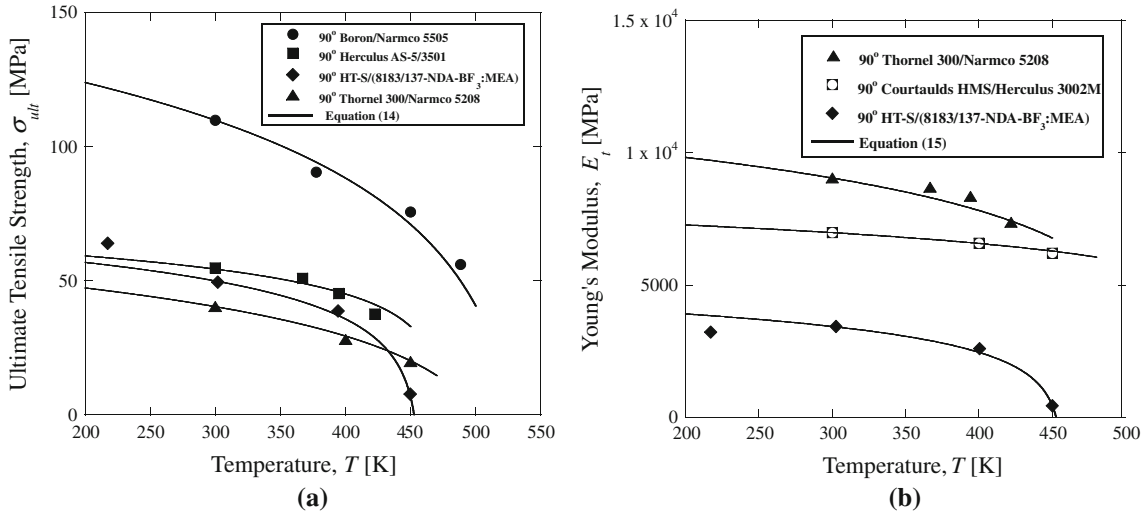

Fig. 6 (**a**) Ultimate tensile strength and (**b**) tensile modulus of different 90° FRP composites as a function of temperature. Experimental data have been extracted from Refs. [17, 18]

Table 5 The experimental information extracted from Hiwa et al. [26] for glass cloth/polyvinyl ester and glass mat/polyvinyl ester used to evaluate the proposed temperature-dependant fatigue damage model

Material at (T (K))			E_c (MPa)								σ_{ult} (MPa)
Cloth (298)			24,000								431
Mat (298)			13,900								251
Material at (T (K))	T_m (K)	K_f	E_f (MPa)	C_E	C_σ	V_f	f^*	σ_{max} (MPa)	R	f (Hz)	nN_f (Cycles)
Cloth (298)	433	0.5	78,400	0.1	0.2	0.48	0.5	130	0	16.7	67,000
Cloth (323)	433	0.5	78,400	0.1	0.2	0.48	0.3	130	0	16.7	52,000
Cloth (343)	433	0.5	78,400	0.1	0.2	0.48	0.1	130	0	16.7	45,500
Mat (298)	433	0.375	78,400	0.1	0.2	0.35	0.5	90	0	16.7	98,939
Mat (373)	433	0.375	78,400	0.1	0.2	0.35	0.3	90	0	16.7	95,000
Mat (423)	433	0.375	78,400	0.1	0.2	0.35	0.1	90	0	16.7	16,000

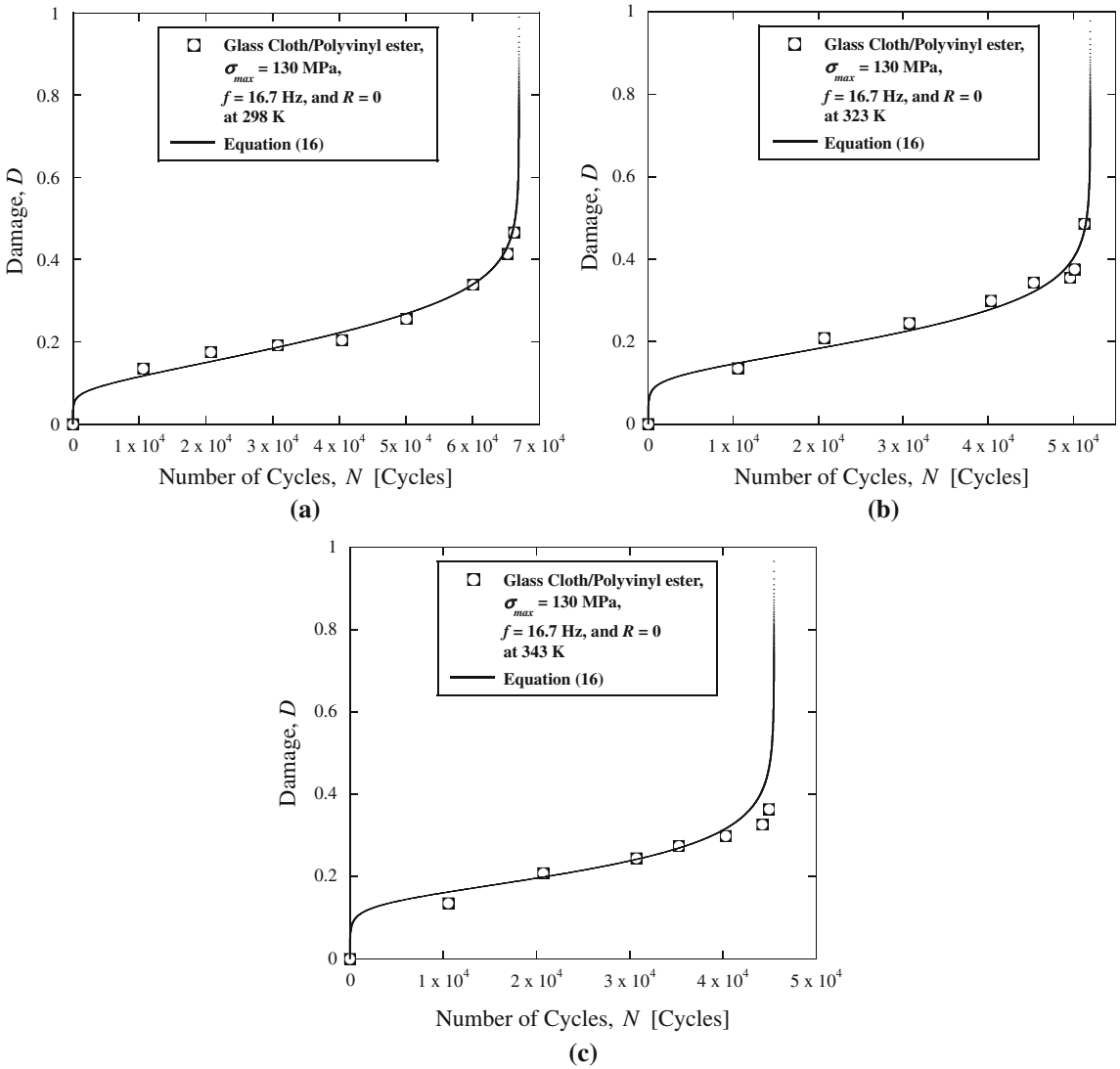

Fig. 7 Fatigue damage of glass cloth/polyvinyle ester versus number of cycles under $\sigma_{max} = 130$ MPa, $f = 16.7$ Hz and $R = 0$ at 298, 323 and 343 K. Experimental data have been extracted from Ref. [26]

Ref. [26] and listed in Table 5. Figures 7 and 8 present the evaluation of fatigue damage over life cycles at various temperatures. These figures show the fact that the experimental data and predicted damage values using the proposed damage model are in good agreement.

Discussion of results

Temperature and the monotonic properties

As illustrated in Figs. 3, 4, 5 and 6, the curves generated using the proposed σ_{ult}–T and E–T relations show a good correlation with experimental data. To more clearly illustrate the deviation of the experimental data from the models, the diagrams have not been shown from 0 to T_m. It is obvious that the models can predict the behaviour of the mechanical properties in the entire temperature range.

To formulate and calibrate the temperature dependency of the monotonic properties, various sets of experimental data were extracted from four different references [17–20]. The type of plies and laminates used in these references included 0°, $[0/90]_{4S}$, $[0/+45/90/-45]_{2S}$ and 90°. The types of materials used as the specimen also included boron/epoxy, S-glass/epoxy, E-glass/epoxy, alumina/PEEK, graphite/PEEK and different types of graphite/epoxy composites. One of the advantages and strong points of the proposed σ_{ult}–T and E–T relations is that they can successfully be applied to all the specimens with a variety of types and laminate structures.

Based on the calculated results presented in Figs. 3, 4, 5 and 6, the effect of temperature on 0° plies is less than

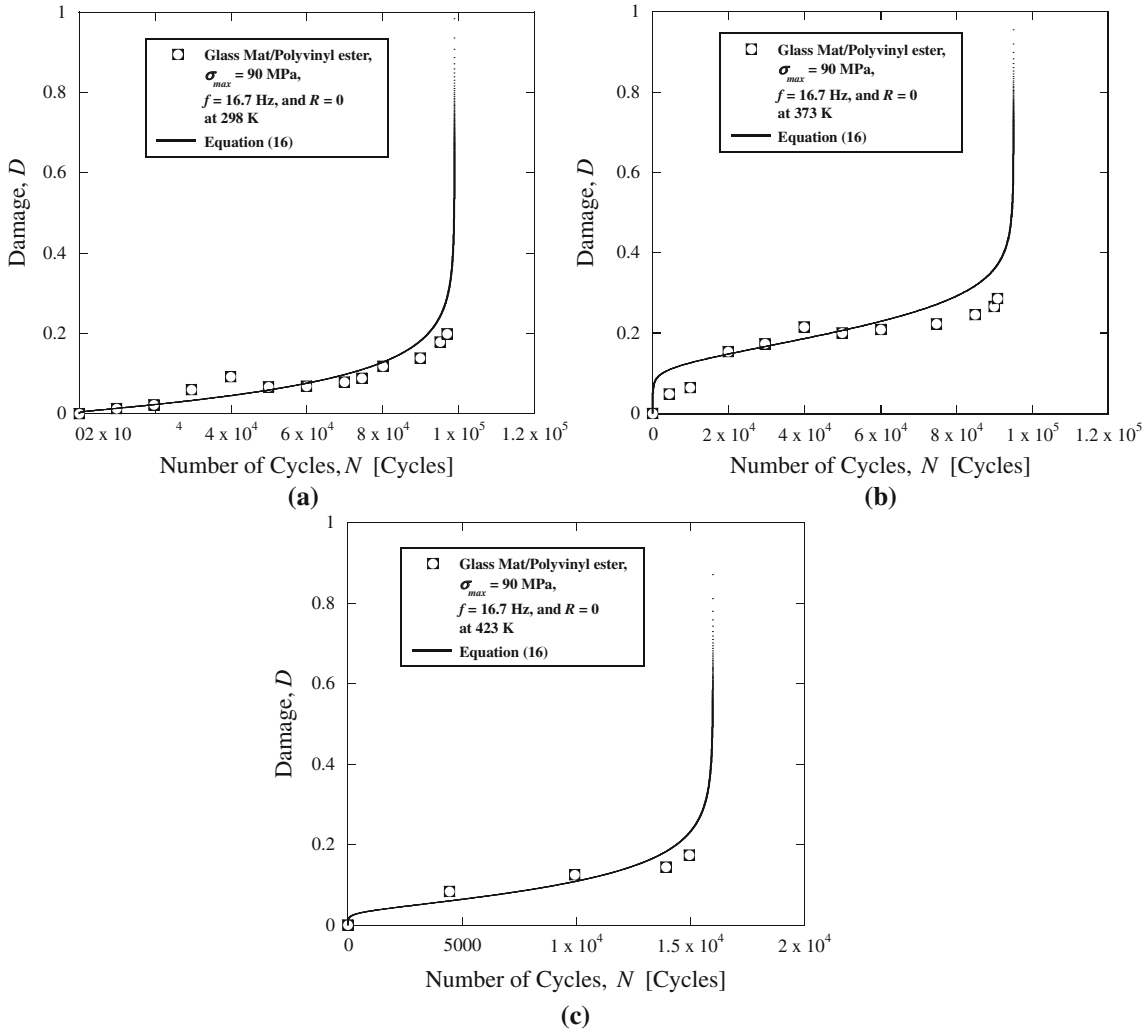

Fig. 8 Fatigue damage of glass mat/polyvinyle ester versus number of cycles under $\sigma_{max} = 90$ MPa, $f = 16.7$ Hz and $R = 0$ at 298, 373 and 343 K. Experimental data have been extracted from Ref. [26]

$[0/90]_{4S}$, $[0/+45/90/-45]_{2S}$ and 90°, where as 90° lay-ups have the highest sensitivity to temperature changes. The sensitivity to temperature is also different between the ultimate tensile strength and Young's modulus of a composite material. Figures 3, 4, 5 and 6 illustrate the fact that the effect of temperature on the ultimate tensile strength is more pronounced than that on Young's modulus. In the proposed temperature-dependent formulation, the sensitivity of the mechanical properties to temperature is evaluated based on constants C_σ and C_E. The bigger their values are, the higher temperature sensitivity is, and vice versa.

Temperature and fatigue damage

To evaluate fatigue damage Eq. 16 as the proposed fatigue damage model, six sets of *D*–*N* data were extracted from the literature. The data had been obtained by fatigue tests with the loading frequency of 16.7 Hz and the stress ratio of 0. The tests were performed on glass cloth/polyvinyl ester with the maximum stress of 130 MPa at RT (298 K), 323 and 343 K and the glass mat/polyvinyl ester with the maximum stress of 90 MPa at RT (298 K), 373 and 423 K. The *D*–*N* data modelled with Eq. 16 have been illustrated in Figs. 7 and 8. In all the graphs of the figures, the experimental data show a good correlation with the model.

The main point concluded from the *D*–*N* graphs is that, with increasing temperature, the cumulative fatigue damage is increased. The damage increase is due to the damage growth in each of the three regions of I (matrix cracking), II (fibre/matrix interface cracking) and III (fibre breakage). To understand the point more clearly, as an example, all the three *D*–*N* curves for the glass cloth/polyvinyl ester at 298, 323 and 343 K are shown together in Fig. 9. In this figure, as temperature increases, fatigue life decreases, and fatigue damage in each of the three regions of I, II and III

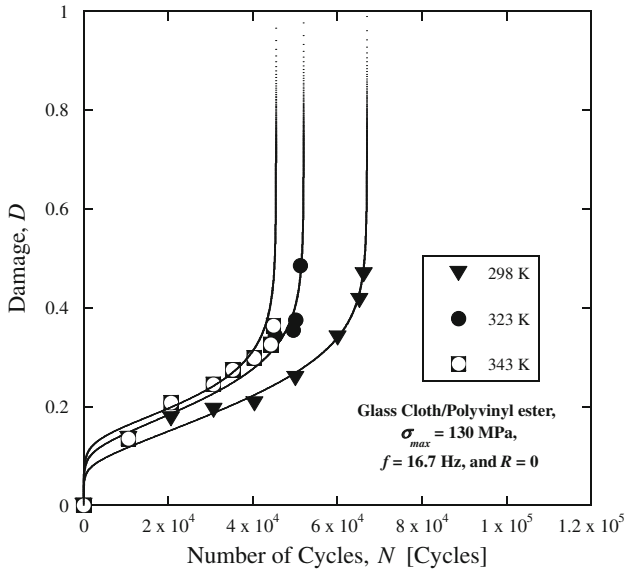

Fig. 9 Fatigue damage of glass cloth/polyvinyle ester versus number of cycles under $\sigma_{max} = 130$ MPa, $f = 16.7$ Hz and $R = 0$ at 298, 323 and 343 K. Experimental data have been extracted from Ref. [26]

increases. Therefore, the overall cumulative fatigue damage increases.

Conclusions

The cumulative fatigue damage models of Ramkrishnan–Jayaraman and Varvani-Farahani–Shirazi were further developed based on the temperature-dependent parameters of $\sigma_{ult}(T)$ and $E(T)$ to assess the fatigue damage of FRP composites at various temperatures. To characterize the temperature-dependent parameters, a shifting factor concept was introduced, which is able to predict the mechanical properties of 0°, 90° and the intermediate composite lay-ups.

The proposed shift factor equation is advantageous over the WLF and the Arrhenius equations. These two equations are merely suitable for bulk polymers, and they are applicable at temperatures above the glass transition temperature of the polymer. However, the proposed shift factor equation is applicable for laminated FRP composites at operating temperatures between 0 K and the polymer melting point (T_m).

Using the proposed shift factor, monotonic mechanical properties of laminated FRP composites including E and σ_{ult} were formulated as a function of temperature. Using the formulae, the temperature-dependent fatigue damage equation was proposed. The model was evaluated using six sets of damage data extracted from the literature. Comparison of the D–N curve predicted using Eq. 16 and the D–N experimental values were found to be in good agreement.

Acknowledgements The financial support by Natural Science and Engineering Research Council of Canada (NSERC) is very much appreciated.

References

1. Degrieck J, Paepegem WV (2001) Appl Mech Rev 54(4):279
2. Epaarachchi JA, Clausen PD (2000) In: Hui D (ed) Proceeding of the seventh international conference on composite engineering (ICCE/7). Denver, Colorado, p 211
3. Ellyin F, El-Kadi H (1990) Compos Struct 15(1):61
4. Hashin Z, Rotem A (1973) J Compos Mater 7(4):448
5. Ramakrishnan V, Jayaraman N (1993) J Mater Sci 28:5592. doi: 10.1007/BF00367835
6. Varvani-Farahani A, Shirazi A (2007) J Reinf Plast Compos 26(13):1319
7. Hwang W, Han KS (1986) J Compos Mater 20(2):125
8. Whitworth HA (2000) Compos Struct 48(4):261
9. Schön J (2000) Compos Sci Technol 60(4):553
10. Biner SB, Yuhas VC (1989) J Eng Mater Technol 111(4):363
11. Reifsnider KL (1986) Eng Fract Mech 25(5–6):739
12. Nielsen LE (1974) Mechanical properties of polymers and composites, vol 1. Marcel Dekker Inc., New York
13. Ward IM, Sweeney J (2004) An introduction to the mechanical properties of solid polymers, 2nd edn. Wiley, New York
14. Miyano Y, Nakada M, Kudoh H (2000) J Compos Mater 34(7):538
15. Aklonis JJ, MacKnight WJ, Shen M (1972) Introduction to polymer viscoelasticity. Wiley, New York
16. Thorne JL (1996) Technology of thermoforming. Hanser/Gardner Publications Inc., Cincinnati, USA
17. Shen C-H, Springer GS (1977) J Compos Mater 11(1):2
18. Shen C-H, Springer GS (1977) J Compos Mater 11(3):250
19. Reed RP, Golda M (1994) Cryogenics 34(11):909
20. Jen M-HR, Tseng Y-C, Kung H-K, Huang J-C (2008) Composites B 39(7–8):1142
21. Hofer KE, Jr, Larsen D, Humphreys VE (1974) Development of engineering data on the mechanical and physical properties of advanced composites materials, Technical Report AFML-TR-72-205, Part II. Air force Materials Laboratory, Air force System Command, Wright-Patterson Air force Base, Dayton, OH
22. Husman GE (1976) In: Presented at the mechanics of composites review. Bergamo Centre, Dayton, OH
23. Hertz J (1973) Investigation into the high-temperature strength degradation of fibre-reinforced resin composite during ambient aging, Report No. GDCA-DBG73-005, Contract NAS8-27435. Convair Aerospace Division, General Dynamics Corporation
24. Browning CE, Husman GE, Withney JM (1976) Moisture effects in epoxy matrix composites, vol 617. Composite Materials: Testing and Design. Philadelphia, ASTM, STP
25. Kaminski BE (1973) Effects of specimen geometry on the strength of composite materials. Analysis of the test methods for high modulus fibres and composites, vol 521. Philadelphia, ASTM STP
26. Hiwa C, Ueda S-I, Nakagawa T (1986) Mem Fac Eng Kobe Univ 33:15